

# Application of the Yin-Yang grid to a thermal convection of a Boussinesq fluid with infinite Prandtl number in a three-dimensional spherical shell

Masaki Yoshida and Akira Kageyama

Earth Simulator Center, Japan Agency for Marine-Earth Science and Technology, Yokohama, Japan

Received 12 March 2004; revised 30 April 2004; accepted 18 May 2004; published 25 June 2004.

[1] A new numerical finite difference code has been developed to solve a thermal convection of a Boussinesq fluid with infinite Prandtl number in a three-dimensional spherical shell. A kind of the overset (Chimera) grid named “Yin-Yang grid” is used for the spatial discretization. The grid naturally avoids the pole problems which are inevitable in the latitude-longitude grids. The code is applied to numerical simulations of mantle convection with uniform and variable viscosity. The validity of the Yin-Yang grid for the mantle convection simulation is confirmed.

*INDEX TERMS:* 8120 Tectonophysics: Dynamics of lithosphere and mantle—general; 8121 Tectonophysics: Dynamics, convection currents and mantle plumes; 8162 Tectonophysics: Rheology—mantle. *Citation:* Yoshida, M., and A. Kageyama (2004), Application of the Yin-Yang grid to a thermal convection of a Boussinesq fluid with infinite Prandtl number in a three-dimensional spherical shell, *Geophys. Res. Lett.*, *31*, L12609, doi:10.1029/2004GL019970.

## 1. Introduction

[2] From the middle of 1980s, numerical simulation codes for the thermal convection with infinite Prandtl number in three-dimensional (3-D) spherical shells have been developed to solve the mantle convection of terrestrial planets. The discretization methods employed in these codes can be divided into three categories; the spectral method [Machetel *et al.*, 1986; Glatzmaier, 1988; Bercovici *et al.*, 1989; Zhang and Yuen, 1995; Harder and Christensen, 1996], the finite element (FE) method [Baumgardner, 1985; Bunge and Baumgardner, 1995; Zhong *et al.*, 2000; Tabata and Suzuki, 2000; Richards *et al.*, 2001], and the finite volume (FV) method [Ratcliff *et al.*, 1996; Iwase, 1996]. The spectral method, which can be an effective method for spherical flows [e.g., Fornberg, 1996; Fornberg and Merrill, 1997], had found to be unsuitable to mantle convection simulations because of intense spatial variation of the viscosity of mantle rock. A new method based on multilevel wavelet algorithm [Vasilyev *et al.*, 1997] can treat the spatially localized physical properties and has a great potential usefulness in mantle convection simulations. Its application to a spherical shell model is, however, still remains a challenging task. Among the grid-based FE, FV and finite difference (FD) schemes, the FV and FD methods are more desirable than FE for massively parallel vector computers because of their feasibility of optimization. Another advantage of the FD method is its flexibility; the

extension to higher-order schemes, which might be important to obtain accurate solutions of thermal convection with very large Rayleigh numbers [e.g., Larsen *et al.*, 1997], is relatively easy.

[3] One of the most popular computational grids in the spherical polar coordinates ( $r$ ,  $\theta$ ,  $\phi$ ) is latitude-longitude ( $\theta$ ,  $\phi$ )-grid, which is defined by intersections of latitude and longitude circles on a sphere (Figure 1a). It is widely recognized that the ( $\theta$ ,  $\phi$ )-grid has the “pole problems” that refer to two different kinds of difficulty in numerical calculations; one is the coordinate singularity on the poles ( $\theta = 0, \pi$ ); and the other is the grid convergence near the poles. The pole problems have been considered as serious difficulties in the community of mantle convection simulation. To avoid the coordinate singularity, special cares have to be taken. In the FV method, for example, all the physical variables are arranged not to reside on the pole grids [Ratcliff *et al.*, 1996; Iwase, 1996]. The problem of the grid convergence is more serious than the coordinate singularity: It causes not only the grid redundancy, but also the severe restriction on the time-step due to the Courant-Friedrichs-Levy (CFL) condition. In the ( $\theta$ ,  $\phi$ )-coordinates, the grid spacing on the spherical surfaces is extremely non-uniform as Figure 1a shows. The largest grid spacing  $\Delta X$  is given in the equator;  $\Delta X = 2\pi/N_\phi$ , where  $N_\phi$  is the grid number in the  $\phi$ -direction, while the smallest grid spacing  $\Delta x$  is given at the nearest latitude to the poles;  $\Delta x = r \sin(\pi/N_\theta) \times (2\pi/N_\phi) \sim 2\pi^2 r / (N_\theta N_\phi)$ , where  $N_\theta$  is the grid number in the  $\theta$ -direction. So the ratio  $\Delta X/\Delta x \sim N_\theta/\pi$  increases in proportional to the grid number. This means that the time-step restriction becomes extremely severe for large scale simulations with fine grids. To avoid the impractically small time-step, one has to invoke quasi-uniform grid spacing over the sphere. The FE based codes referred above employed carefully designed grid cells for that purpose. For example, a FE mantle convection code named CitcomS has nearly uniform resolution in both polar and equatorial regions [Zhong *et al.*, 2000]. However, a FD or FV based mantle convection code that overcomes both of the pole singularity and the grid convergence have not been reported so far.

[4] Here we employ a new grid system for spherical shell geometry, named “Yin-Yang grid”, which has been proposed recently by A. Kageyama and T. Sato (The “Yin-Yang grid”: An overset grid in spherical geometry, submitted to *Geochemistry, Geophysics, Geosystems*, 2004, hereinafter referred to as Kageyama and Sato, submitted manuscript, 2004). The Yin-Yang grid is composed of two component grids that have exactly the same shape and size (Figure 1b). They partially overlap each other on their boundaries

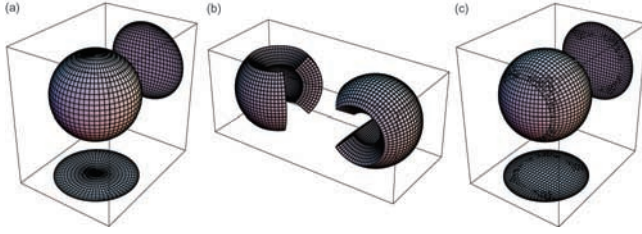


**Figure 1.** The latitude-longitude  $(\theta, \phi)$ -grid and new spherical overset grid named “Yin-Yang grid”. (a) The  $(\theta, \phi)$ -grid. (b) Two component grids of the Yin-Yang grid. They are identical (same shape and size); the low latitude part  $(\pi/4 \leq \theta \leq 3\pi/4, -3\pi/4 \leq \phi \leq 3\pi/4)$  of the  $(\theta, \phi)$ -grid. (c) They partially overlap each other at their interface to cover a spherical surface in pair (see text and Kageyama and Sato (submitted manuscript, 2004) for details).

(Figure 1c). Following the overset (Chimera) grid method [Cheshire and Henshaw, 1990], data on the boundaries of the component grids are matched by interpolation. A component grid of the Yin-Yang grid is actually a low latitude part of the  $(\theta, \phi)$ -grid. As it is apparent in Figure 1b, the Yin-Yang grid has neither a coordinate singularity, nor grid convergence; the grid spacings are quasi-uniforms on the sphere (see Kageyama and Sato (submitted manuscript, 2004) for more details on this grid).

[5] In this paper, we apply the Yin-Yang grid for the numerical simulation of mantle convection. To confirm the validity of the Yin-Yang grid, we have performed benchmark tests with published numerical codes for steady convections. We also apply the Yin-Yang grid for time-dependent mantle convections with uniform and variable viscosity.

## 2. Model and Numerical Methods

[6] We model the mantle convection as a thermal convection of a Boussinesq fluid with infinite Prandtl number heated from bottom of a spherical shell. The ratio of the inner radius ( $r = r_0$ ) and the outer radius ( $r = r_1$ ) is 0.55. The normalization factors for the non-dimensionalization of the length, velocity, time and temperature are  $\hat{r}_1 = 6371$  km (the Earth’s radius),  $\hat{\kappa}/\hat{r}_1$ ,  $\hat{r}_1^2/\hat{\kappa}$  and  $\Delta\hat{T} = \hat{T}_{bot} - \hat{T}_{top}$ , respectively, where  $\hat{\kappa}$  is the thermal diffusivity, and  $\hat{T}_{bot}$  and  $\hat{T}_{top}$  are the temperatures on the bottom and top surfaces. The hat stands for dimensional quantity. The non-dimensional equations of mass, momentum, and energy conservation governing the thermal convection are,

$$\nabla \cdot \mathbf{v} = 0, \quad (1)$$

$$0 = -\nabla p + \nabla \cdot (\eta \dot{\epsilon}) + Ra \zeta \mathbf{e}_r, \quad (2)$$

$$\partial_t T = \nabla^2 T - \mathbf{v} \cdot \nabla T, \quad (3)$$

where  $\mathbf{v}$  is the velocity vector,  $p$  the dynamic pressure,  $T$  the temperature,  $t$  the time,  $\dot{\epsilon}$  the strain-rate tensor, and  $\mathbf{e}_r$  is the unit vector in the  $r$ -direction. The constant parameter  $\zeta$  is  $(\hat{d}/\hat{r}_1)^3 = 0.45^3$ , where  $\hat{d} = \hat{r}_1 - \hat{r}_0$  is the thickness of the

shell, 2890 km (the Earth’s mantle). We assume that viscosity  $\eta$  depends only on temperature;

$$\eta(T) = \eta_{ref} \exp[-E(T - T_{ref})], \quad (4)$$

where  $T_{ref}$  is the reference temperature, and  $\eta_{ref}$  is the reference viscosity at  $T_{ref}$ . The parameter  $E$  denotes the degree of viscosity contrast between the top and bottom surfaces. The viscosity contrast across the spherical shell is defined by  $\gamma_\eta \equiv \eta(T_{top})/\eta(T_{bot}) = \exp(E)$ . The Rayleigh number is defined by  $Ra \equiv \hat{\rho} \hat{g} \hat{\alpha} \Delta\hat{T} \hat{d}^3 / \hat{\kappa} \eta_{ref}$ , where  $\hat{\rho}$  is the density,  $\hat{g}$  the gravitational acceleration, and  $\hat{\alpha}$  is the thermal expansivity. The mechanical boundary conditions at the top and bottom surface are impermeable and stress-free. The boundary conditions for  $T$  are  $T_{bot} = 1$  and  $T_{top} = 0$ .

[7] We use the collocated grid method [e.g., Ferziger and Perić, 2002]; all the primitive variables,  $\mathbf{v}$ ,  $p$  and  $T$ , are defined on the same grid points. Equations (1)–(3) are solved by the FD discretization with second-order accuracy. The SIMPLER algorithm [Patankar, 1980; Ferziger and Perić, 2002] is applied to solve  $\mathbf{v}$  and  $p$  from equations (1) and (2). The Crank-Nicolson method is used in equation (3) for the time stepping. The upwind difference method is applied for the advection term in equation (3). With the Yin-Yang grid method, we simultaneously solve equations (1)–(3) for each component grid. We use a successive over-relaxation (SOR) method as the iterative solver required in the SIMPLER algorithm and the energy equation. The horizontal boundary values of each component grid are determined by linear interpolation from the other component grid. The interpolation is taken at each SOR iteration. (We confirmed that the interpolation procedure has no numerical mischief on the calculations.) The grid size is  $102 \times 102 \times 204$  (in  $r$ -,  $\theta$ -, and  $\phi$ -directions). We have confirmed that this size is enough to resolve all the convections studied in this paper. Time development of the convection is calculated until averaged quantities, such as Nusselt number and root-mean-square velocity, become stationary.

## 3. Benchmark Tests

[8] The thermal convection in the spherical shell with infinite Prandtl number has two stable solutions with polyhedral symmetry when the Rayleigh number is low [e.g., Schubert, 2001]. The two solutions are found by linear theory [Busse, 1975; Busse and Riahi, 1982] and confirmed by numerical simulations [Bercovici et al., 1989; Ratcliff et al., 1996]: One solution is a convection with the tetrahedral symmetry which has four upwellings; the other has the cubic symmetry with six upwellings. To confirm these symmetric solutions and their stabilities, we performed two simulations with different initial conditions of temperature field;  $T(r, \theta, \phi) = T_{cond}(r) + T_{prtb}(r, \theta, \phi)$ , where  $T_{cond}(r) = r_0(r_1 - r)/r(r_1 - r_0)$  is the purely conductive profile, i.e.,  $\nabla^2 T_{cond}(r) = 0$ , with the thermal boundary conditions given above. The perturbation term  $T_{prtb}(r, \theta, \phi)$  is given by,

$$T_{prtb}(r, \theta, \phi) = \lambda [Y_3^2(\theta, \phi) + \Omega(\theta, \phi)] \sin \pi(r - r_0), \quad (5)$$

**Table 1.** The Benchmark Test of Nusselt Numbers at the Top Surface ( $Nu$ ) and RMS Velocity ( $V_{rms}$ ) of the Entire Mantle<sup>a</sup>

T/C	$Ra_{1/2}$	$\gamma_\eta$	$Nu$								$V_{rms}$				
			G188 (SP)	Br89 (SP)	HC96 (SP)	Rt96 (FV)	Iw96 (FV)	Zh00 (FE)	TS00 (FE)	Rc01 (FE)	YK04 (FD)	Rt96 (FV)	Iw96 (FV)	TS00 (FE)	YK04 (FD)
T	2.0e3	1	-	2.2507	-	2.1740	2.18	2.218	2.2432	-	2.2025	12.14	12.4710	12.5739	12.1246
T	7.0e3	1	-	3.4657	3.4957	3.4423	3.45	3.519	3.6565	3.4160	3.4430	32.19	32.4173	32.9360	32.0481
T	1.4e4	1	4.2820	-	4.2818	4.2028	-	-	-	4.2250	4.2395	50.27	-	-	50.0048
T	7.0e3	20	-	-	-	3.1615	-	-	-	-	3.1330	25.69	-	-	26.1064
C	3.5e3	1	-	2.7954	-	2.8306	2.80	-	-	-	2.8830	18.86	-	-	18.4801
C	7.0e3	1	-	-	-	3.5806	3.54	-	-	-	3.5554	30.87	-	-	30.5197
C	1.4e4	1	-	-	-	4.4449	-	-	-	-	4.4231	48.75	-	-	48.1082
C	7.0e3	20	-	-	-	3.3663	-	-	-	-	3.3280	25.17	-	-	25.3856

<sup>a</sup>“T/C” denotes the tetrahedral (“T”) or cubic (“C”) symmetric solutions. The abbreviated code names “G188” is for *Glatzmaier* [1988], “Br89” *Bercovici et al.* [1989], “HC96” *Harder and Christensen* [1996], “Rt96” *Ratcliff et al.* [1996], “Iw96” *Iwase* [1996], “Zh00” *Zhong et al.* [2000], “TS00” *Tabata and Suzuki* [2000], “Rc01” *Richards et al.* [2001], and “YK04” is for our code. The “SP” in parentheses under each code name denotes spectral method, and see text for “FV”, “FE” and “FD”. (Note that, in this benchmark test, the normalization factor used to non-dimensionalize the length is the Earth’s radius  $\hat{r}_1$ , not  $\hat{d}$ .)

for the tetrahedral symmetric solution, and

$$T_{prtb}(r, \theta, \phi) = \lambda \left[ Y_4^0(\theta, \phi) + \frac{5}{7} Y_4^4(\theta, \phi) + \Omega(\theta, \phi) \right] \times \sin \pi(r - r_0), \quad (6)$$

for the cubic symmetric solution, where  $Y_\ell^m(\theta, \phi)$  is the fully normalized spherical harmonic functions of degree  $\ell$  and order  $m$ . The  $Y_\ell^m(\theta, \phi)$  terms in equations (5) and (6) determine the solution’s symmetry. The other term  $\Omega(\theta, \phi)$  is for secondary perturbation. We set  $\Omega(\theta, \phi) = \omega \sum_{\ell=1}^{12} \sum_{m=0}^{\ell} Y_\ell^m(\theta, \phi)$ .

[9] We have performed benchmark tests with published numerical mantle convection codes that employed various numerical schemes. Following *Richards et al.* [2001] and *Ratcliff et al.* [1996], we performed simulations of uniform ( $\gamma_\eta = 1$ ) and variable ( $\gamma_\eta = 20$ ) viscosity convections with both the tetrahedral and cubic steady symmetries when  $\lambda = 10^{-1}$  and  $\omega = 0$  (i.e., no secondary perturbations). The Rayleigh number  $Ra_{1/2}$  is defined by the reference viscosity  $\eta_{ref}$  at  $T_{ref} = 0.5$  [*Ratcliff et al.*, 1996]. Nusselt number at the surface and root-mean-square velocity of entire domain were calculated on convections at  $Ra_{1/2} = 2.0 \times 10^3 \sim 1.4 \times 10^4$ . The results of the benchmark tests are summarized in Table 1. In spite of the differences of the discretization methods, numerical techniques, and number of grid points among the codes, we found that the results from our code agree well with them within a few percent or even better and confirmed the validity of our code.

#### 4. Unsteady Convection Problems

[10] The steady convections become time-dependent when the Rayleigh number is increased. Since the Earth’s mantle is obviously time-dependent convection with high Rayleigh number, the transition of convection from steady to unsteady state is important. We tried a series of simulations with various  $Ra_{bot}$  (the Rayleigh number defined by the reference viscosity at the bottom surface, i.e.,  $T_{ref} = T_{bot}$ ) from the critical number for convection onset ( $\approx 712$ ) [*Ratcliff et al.*, 1996] to  $10^5$ . The perturbation amplitudes  $\lambda$  and  $\omega$  are taken to be  $10^{-1}$  and  $10^{-3}$ , respectively. Shown in Figure 2 are the iso-surfaces of temperature at  $Ra_{bot} = 10^4$  and  $10^5$  after 200,000 time-steps. Figures 2a and 2b indicate that, at  $Ra_{bot} = 10^4$ , the convection patterns are in steady

states, maintaining each symmetry, in spite of the existence of the secondary perturbations in the initial conditions. This is consistent with earlier results [*Bercovici et al.*, 1989; *Ratcliff et al.*, 1996] in which the secondary perturbation was not explicitly imposed, i.e.,  $\omega = 0$ , though.

[11] When  $Ra_{bot} = 10^5$ , the convection patterns become weakly time-dependent. The geometrical symmetry in this Rayleigh number is broken. This disagrees with the result of *Ratcliff et al.* [1996]. Notice that, in the right panel of Figure 2b, all the six upwelling plumes have the same diameters in our results. The corresponding case by *Ratcliff et al.* [1996], in which a FV scheme on the  $(\theta, \phi)$ -grid is used, shows a symmetric pattern about equator and appears

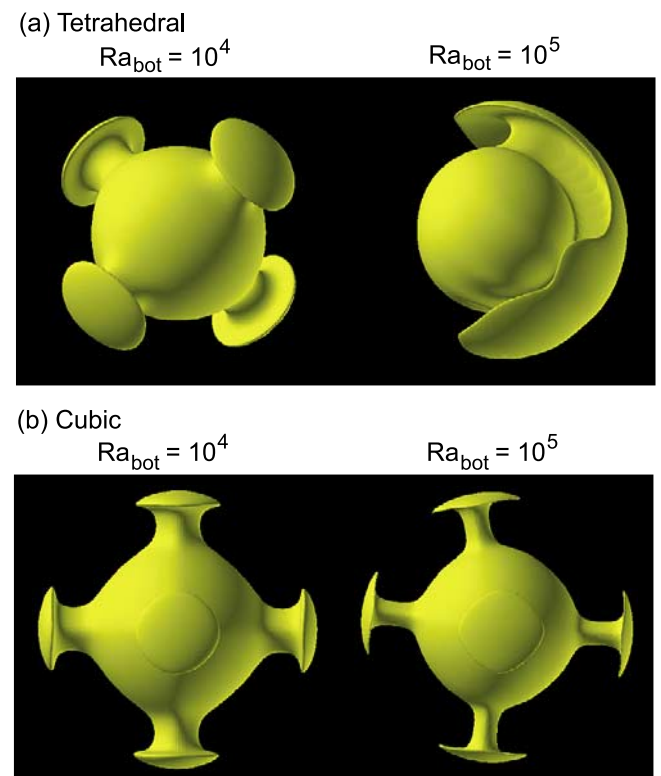


**Figure 2.** The iso-surface renderings of temperature ( $T = 0.4$ ) started from the initial conditions of (a) tetrahedral, and (b) cubic symmetries. The left and right panels on each figure show the cases at  $Ra_{bot} = 10^4$  and  $10^5$ , respectively.

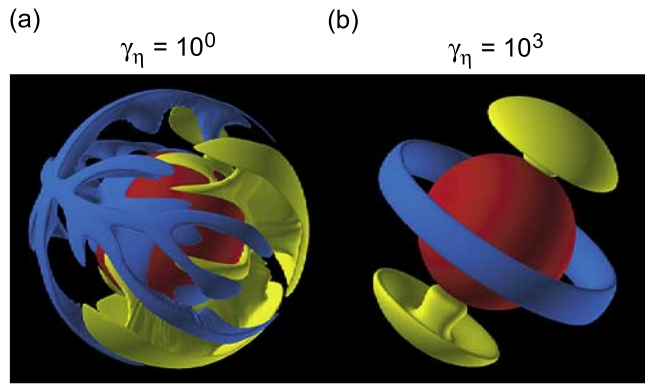


**Figure 3.** The iso-surface renderings of residual temperature  $\delta T$  (i.e., the deviation from horizontally averaged temperature at each depth) for the cases at  $\gamma_\eta =$  (a)  $10^0$ , and (b)  $10^3$ . Blue iso-surfaces stand for  $\delta T$  of (a)  $-0.10$ , and (b)  $-0.25$ . Yellow iso-surfaces for  $\delta T$  of (a)  $+0.10$ , and (b)  $+0.25$ . Red spheres indicate the bottom surface of spherical shell.

to remain in a steady state [cf. *Ratcliff et al.*, 1996, Figure 6]. These observations suggest that the low Rayleigh number convections around  $Ra_{bot} = 10^5$  are numerically affected by coordinate singularity and the grid convergence in the  $(\theta, \phi)$ -grid. On the other hand, the pole effects are removed in our code by making use of the Yin-Yang grid.

[12] It is known that variable viscosity with strong temperature dependence induces drastic effects on the convection pattern in 3-D Cartesian model with large aspect ratio and also in the spherical shell model [*Ratcliff et al.*, 1997; *Trompert and Hansen*, 1998]. To confirm this effect in our model, we performed simulations with variable viscosity. Taking equation (5) as the initial temperature perturbation, we first calculated an isoviscous convection at  $Ra_{bot} = 10^6$ . The obtained solution, which is shown in Figure 3a, is strongly time-dependent and exhibits complex feature in contrast to the case at  $Ra_{bot} = 10^5$  (the right panel of Figure 2a). We gradually increased  $\gamma_\eta$  from 1 (isoviscous case) up to  $10^3$ . We obtained a convection regime that has cold and rather thick thermal boundary layer on the top surfaces (Figure 3b). The large aspect ratio of convecting cells in this regime is consistent with the previous results obtained by the 3-D Cartesian model with large aspect ratio as well as spherical shell model with moderately strong temperature-dependence of viscosity ( $\gamma_\eta = 10^3$ ) [*Ratcliff et al.*, 1997]. Our results show that the underlying convection patterns with larger aspect ratio of degree-2 come to dominate. The two cells structure that consists of one sheet-like downwelling along a great circle of spherical shell and two mushroom-shaped upwelling plumes is formed.

## 5. Conclusions and Discussion

[13] We have developed a new numerical simulation code to solve the thermal convection of a Boussinesq fluid with infinite Prandtl number using a second-order FD method on newly devised spherical overset grid named Yin-Yang grid. Our code is powerful and unique FD based code that can solve both the uniform and the strongly variable viscosity convections. The validity of the Yin-Yang grid for the

mantle convection simulation is confirmed by benchmark tests. The Yin-Yang grid is suitable to solve the mantle convection problems because it automatically avoids the pole problems that are inevitable on the  $(\theta, \phi)$ -grid. In the isoviscous case with cubic symmetry at  $Ra_{bot} = 10^5$ , the convection pattern has a weak time-dependence in our Yin-Yang grid, while it was steady with strange asymmetry of the plume sizes between those on the poles and those in the equator in the previous FV scheme on the  $(\theta, \phi)$ -grid. This discrepancy might be a consequence of the grid convergence near poles in the  $(\theta, \phi)$ -grid. Our result implies that large-scale (low degree) convective structures are easily affected numerically by the poles when  $(\theta, \phi)$ -grid is employed. The quadrupole convection patterns is obtained when large viscosity contrast with three orders of magnitude is introduced when  $Ra_{bot} = 10^6$ .

[14] To follow mantle convection for geophysical time-scale ( $\sim 10^8$  years), the computational time-step  $\Delta t$  is critically important in numerical simulations. As we described in section 1, the time-step is determined by the CFL condition by the smallest grid spacing. For  $(\theta, \phi)$ -grid,  $\Delta x (= \Delta x_{\theta\phi})$  is determined by the azimuthal grid spacing at the nearest grids to the pole. On the other hand for the Yin-Yang grid,  $\Delta x (= \Delta x_{YY})$  is determined by the azimuthal grid spacing at  $\theta = \pi/4$  (or  $3\pi/4$ ). Therefore the ratio of time-steps  $\Gamma_t$  between two grids is,

$$\Gamma_t \propto \Delta x_{\theta\phi} / \Delta x_{YY} = \sin(\pi/N_0) / \sin(\pi/4) \approx 1.4\pi/N_0. \quad (7)$$

Taking  $N_0 = 102$  as employed in this paper,  $\Gamma_t \approx 0.04$ . This means that the total computational time is significantly reduced by the factor of 1/25 by making use of the Yin-Yang grid.

[15] **Acknowledgments.** The authors are grateful to Prof. David A. Yuen and an anonymous reviewer for their careful reviews and valuable comments. All the simulations were performed by Earth Simulator, Japan Agency for Marine-Earth Science and Technology.

## References

- Baumgardner, J. R. (1985), Three-dimensional treatment of convective flow in the Earth's mantle, *J. Stat. Phys.*, *39*, 501–511.
- Bercovici, D., G. Schubert, G. A. Glatzmaier, and A. Zebib (1989), Three dimensional thermal convection in a spherical shell, *J. Fluid Mech.*, *206*, 75–104.
- Bunge, H.-P., and J. R. Baumgardner (1995), Mantle convection modeling on parallel virtual machines, *Comput. Phys.*, *9*, 207–215.
- Busse, F. H. (1975), Patterns of convection in spherical shells, *J. Fluid Mech.*, *72*, 67–85.
- Busse, F. H., and N. Riahi (1982), Patterns of convection in spherical shells: Part 2, *J. Fluid Mech.*, *123*, 283–301.
- Chesshire, G., and W. D. Henshaw (1990), Composite overlapping meshes for the solution of partial differential equations, *J. Comput. Phys.*, *90*, 1–64.
- Ferziger, J. H., and M. Perić (2002), *Computational Methods for Fluid Dynamics*, 3rd ed., 423 pp., Springer-Verlag, New York.
- Fornberg, B. (1996), *A Practical Guide to Pseudospectral Methods*, 242 pp., Cambridge Univ. Press, New York.
- Fornberg, B., and D. Merrill (1997), Comparison of finite difference and pseudospectral methods for convective flow over a sphere, *Geophys. Res. Lett.*, *24*(24), 3245–3248.
- Glatzmaier, G. A. (1988), Numerical simulations of mantle convection: Time-dependent, three-dimensional, compressible, spherical shell, *Geophys. Astrophys. Fluid Dyn.*, *43*, 223–264.
- Harder, H., and U. R. Christensen (1996), A one-plume model of Martian mantle convection, *Nature*, *380*, 507–509.
- Iwase, Y. (1996), Three-dimensional infinite Prandtl number convection in a spherical shell with temperature-dependent viscosity, *J. Geomag. Geo-electr.*, *48*, 1499–1514.

- Larsen, T. B., D. A. Yuen, J. M. Moser, and B. Fornberg (1997), A high-order finite-difference method applied to large Rayleigh number mantle convection, *Geophys. Astrophys. Fluid Dyn.*, *84*, 53–83.
- Machetel, P., M. Rabinowicz, and P. Bernardet (1986), Three-dimensional convection in spherical shells, *Geophys. Astrophys. Fluid Dyn.*, *37*, 57–84.
- Patankar, S. V. (1980), *Heat Transfer and Fluid Flow*, 197 pp., Taylor and Francis, Philadelphia, Pa.
- Ratcliff, J. T., G. Schubert, and A. Zebib (1996), Steady tetrahedral and cubic patterns of spherical shell convection with temperature-dependent viscosity, *J. Geophys. Res.*, *101*(B11), 25,473–25,484.
- Ratcliff, J. T., P. J. Tackley, G. Schubert, and A. Zebib (1997), Transitions in thermal convection with strongly variable viscosity, *Phys. Earth Planet. Inter.*, *102*, 201–212.
- Richards, M. A., W.-S. Yang, J. R. Baumgardner, and H.-P. Bunge (2001), Role of a low-viscosity zone in stabilizing plate tectonics: Implications for comparative terrestrial planetology, *Geochem. Geophys. Geosyst.*, *2*(8), Paper number 2000GC000115.
- Schubert, G. (2001), *Mantle Convection in the Earth and Planets*, 940 pp., Cambridge Univ. Press, New York.
- Tabata, M., and A. Suzuki (2000), A stabilized finite element method for the Rayleigh-Benard equations with infinite Prandtl number in a spherical shell, *Comput. Methods Appl. Mech. Eng.*, *190*, 387–402.
- Trompert, R. A., and U. Hansen (1998), On the Rayleigh number dependence of convection with a strongly temperature-dependent viscosity, *Phys. Fluids*, *10*, 351–360.
- Vasilyev, O. V., D. A. Yuen, and Y. Y. Podladchikov (1997), Applicability of wavelet algorithm for geophysical viscoelastic flow, *Geophys. Res. Lett.*, *24*(23), 3097–3100.
- Zhang, S., and D. A. Yuen (1995), The influences of lower mantle viscosity stratification on 3D spherical-shell mantle convection, *Earth Planet. Sci. Lett.*, *132*, 157–166.
- Zhong, S., M. T. Zuber, L. Moresi, and M. Gurnis (2000), Role of temperature-dependent viscosity and surface plates in spherical shell models of mantle convection, *J. Geophys. Res.*, *105*(B5), 11,063–11,082.

---

A. Kageyama and M. Yoshida, Earth Simulator Center, Japan Agency for Marine-Earth Science and Technology, 3173-25 Showa-machi, Kanazawa-ku, Yokohama, Kanagawa 236-0001, Japan. (kage@jamstec.go.jp; myoshida@jamstec.go.jp)